

Article

Numerical Simulation Research on the Temperature Field and Hot Roll Crown Model of Hot Continuous Rolling Mills

Zizheng Li ¹, Sahal Ahmed Elmi ¹, Luxuan Liu ¹, Baoliang Yin ¹, Shuang Kuang ² and Zhenhua Bai ^{1,3,*}

¹ National Engineering Research Center for Equipment and Technology of Cold Strip Rolling, Yanshan University, Qinhuangdao 066004, China; lipoevr@163.com (Z.L.); sahal.ahmed.elmi@gmail.com (S.A.E.); 18813029858@163.com (L.L.); yinbaoliang_2023@163.com (B.Y.)

² Tangshan Iron and Steel Group, Tangshan 063000, China; steelwarrior@163.com

³ State Key Laboratory of Metastable Materials Science and Technology, Yanshan University, Qinhuangdao 066004, China

* Correspondence: bai_zhenhua@aliyun.com

Abstract: Addressing the challenge of roll loss and strip deformation arising from the lack of precise prediction of the roll temperature field in hot tandem rolling mills, this study employs numerical analysis via the finite difference method. Based on the roll temperature field and hot roll crown model, an intelligent support cooling control system for the roll cooling water of hot rolls is established. This system comprehensively considers the direct impact of specific parameters on the roll temperature field in the intricate context of cooling water dynamics. The study focuses on the cyclic superposition effect of rolling coil quantities on the roll temperature field and the resulting hot roll shape, and theoretical calculations along with simulation analyses were conducted using finite element software. Through the integration of field-measured values, the study achieves accurate predictions of the temperature field and hot roll profile for both work rolls and backup rolls.

Keywords: hot rolling; temperature field; numerical simulation; finite difference method



Citation: Li, Z.; Elmi, S.A.; Liu, L.; Yin, B.; Kuang, S.; Bai, Z. Numerical Simulation Research on the Temperature Field and Hot Roll Crown Model of Hot Continuous Rolling Mills. *Metals* **2024**, *14*, 166. <https://doi.org/10.3390/met14020166>

Academic Editor: Zbigniew Pater

Received: 14 December 2023

Revised: 22 January 2024

Accepted: 22 January 2024

Published: 29 January 2024



Copyright: © 2024 by the authors. Licensee MDPI, Basel, Switzerland. This article is an open access article distributed under the terms and conditions of the Creative Commons Attribution (CC BY) license (<https://creativecommons.org/licenses/by/4.0/>).

1. Introduction

Temperature stands out as a crucial parameter in the production process of hot-rolled strip steel [1,2]. The accurate prediction of the temperature field, of the roll, and the contour of the hot roll is paramount in ensuring optimal strip shape, thickness, and width [3,4]. Consequently, calculation of the temperature field of the hot continuous rolling roll and the profile of the hot roll becomes instrumental in achieving effective control over the plate crown and shape [5–7]. The foundational step in resolving the hot roll shape is the computation of the instantaneous temperature field of the roll, followed by deriving the hot roll shape through the integration of temperature and deformation equations. Research efforts are then directed towards understanding the heat conduction process from the temperature of the work roll to that of the support roll. Atack P. A. et al. [8–13] utilized both analytical and finite element methods to compute the roll's temperature field in accordance with theoretical frameworks and practical production scenarios. Jiang et al. [14] proposed a precision online model for the prediction of the thermal crown in an aluminum alloy hot-strip rolling processes. Chen et al. [15] analyzed the influence of work roll shifting and other factors on the roll thermal crown using a finite difference method for roll temperature field modeling. However, during the rolling process, the work rolls and their surrounding environment, including strip steel, air, and cooling water, form a complex heat exchange system. This complexity arises from the need to comprehensively consider factors such as frictional heat between the rolled piece and the work roll, the plastic deformation heat of the rolled piece, air cooling, contact heat conduction between the work roll and the rolled piece, and convective heat transfer between the cooling water and the roll, among other intricate boundary conditions and heat transfer methods [16]. Given these complexities, obtaining

an exact solution through analytical methods for the heat conduction equation is deemed impractical. Consequently, a numerical simulation analysis [17,18] approach employing the finite difference method was adopted, focusing on the temperature field of the roll. This approach takes into account specific parameters within the complex state of the cooling water and the intelligent control system for roll segmental cooling. Validation is conducted through comparison with finite element method results and actual production data [19]. Simultaneously, the impact of an increasing number of rolled coils on the temperature field and hot roll shape of the roll is considered. The result is the development of a calculation model for the temperature field and hot roll shape that is adaptable to various working conditions. Furthermore, this comprehensive approach enhances our understanding of the complex interplay between cooling strategies, roll temperature, and resulting roll shape in the hot continuous rolling process. At the same time, it provides prediction means and methods for abnormal roll wear and strip shape defects caused by roll hot crown.

2. Materials and Methods

2.1. Model Parameter Settings

To provide a practical illustration and facilitate comparison, a specific frame was selected from a finishing rolling unit in a hot rolling production line at a steel plant. The roll size parameters include the length of the work roll body $L_{w1} = 2350$ mm and the length of the support roll body $L_{b1} = 2050$ mm. The on-site roll temperature data was obtained through collaboration between the school and the enterprise. A contact roll temperature measurement device was utilized in our laboratory, and during the reheating process of the rolls on site, the actual roll temperature was measured with the assistance of a handheld thermometer. Table 1 presents the physical parameters of the roll in specification rolling based on the material's physical properties [20].

Table 1. Physical parameters of roll.

Roll-Specific Heat Capacity/ (J/°C·kg)	Roll Density/ (kg/m ³)	Thermal Conductivity/ (W/m·°C)	Thermal Expansion Coefficient/ (°C ⁻¹)	Poisson Ratio
460	7.38×10^{-6}	0.029	12×10^{-6}	0.287

The initial temperature condition for calculating the temperature field of the work roll, as determined according to the actual situation on site, is the initial temperature of the work roll. The flow velocity was generally between 1.0 and 1.5 m/s, and under the boundary temperature conditions in Table 2, the temperature field and hot roll shape of the rolled strip specification were 29.72×1500 mm.

Table 2. Boundary temperature parameters.

Rolled Piece Temperature/(°C)	Cooling Water Temperature/(°C)	Bearing Temperature/(°C)	Air Temperature/(°C)
900	60	35	25

Utilize DEFORM v11 finite element software to compute the roll temperature field during its operation in cooling water. To maintain symmetry during the rolling process, a 1/2 model of the working roll was established, and the roll mesh was subdivided into tetrahedral elements, as depicted in Figure 1. Aligning with actual working conditions, boundary conditions for the work rolls were defined, encompassing convective heat transfer between the roll and the cooling water injection area, as well as heat conduction between the roll and the rolled piece. Subsequently, the simulation captures the temperature field distribution of the work rolls throughout the rolling process, establishing a transient finite element model for the roll [21].

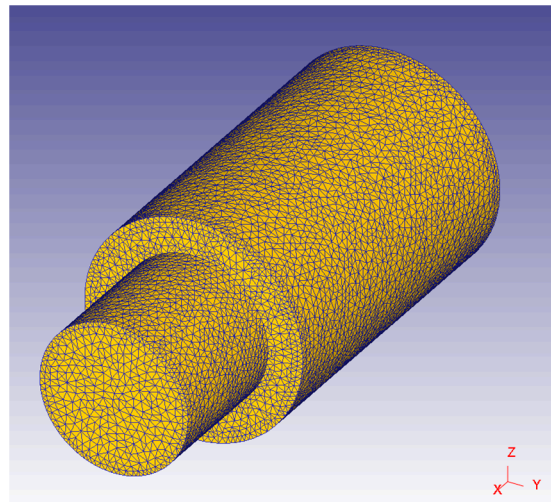


Figure 1. Work roll finite element model.

2.2. Establishment of Basic Requirements for Roller Temperature Field

Assuming that the roll is an infinitely long cylinder, its temperature is symmetrically distributed relative to its rotation. Additionally, the thermal oscillations it undergoes manifest in two directions: symmetrical, and circumferential. Numerous experiments and studies have demonstrated that due to the temperature field fluctuation occurring primarily in the thin surface layer of the roll, temperature fluctuation in the circumferential direction within the symmetry perpendicular to the axis is almost negligible. Consequently, the temperature field of the roll can be simplified to a two-dimensional problem [22].

The heat conduction equation of the roll [23] is simplified as:

$$\rho c \frac{\partial T}{\partial t} = \lambda \frac{\partial^2 T}{\partial r^2} + \frac{\lambda}{r} \left(\frac{\partial T}{\partial r} \right) + \lambda \frac{\partial^2 T}{\partial z^2} \quad (1)$$

where T is roll temperature; t is time; c is roll-specific heat; ρ is roll density; λ is roll thermal conductivity; r is the radial coordinate value of the roll; z is the axial coordinate value of the roll.

By using the finite difference method, the roll is divided into several equal grids. The grid division is shown in Figure 2, where $r(j)$ is the radial coordinate and $z(i)$ is the axial coordinate. The origin is situated at the center of gravity of the roll. The middle section of the body is symmetrically distributed, prompting the selection of a quarter section through the roll axis as the focal point for research. Subsequently, a differential scheme for the temperature distribution across the entire grid system is established. Equation (2) is the differential expression of the roll thermal balance equation [24].

$$\left[\frac{T_{i,j+1} - 2T_{i,j} + T_{i,j-1}}{(\Delta r)^2} + \frac{T_{i,j+1} - T_{i,j-1}}{2r_0 \Delta r} + \frac{T_{i+1,j} - 2T_{i,j} + T_{i-1,j}}{(\Delta z)^2} \right] = \frac{\rho C_p}{k} \left(\frac{T_{i,j}^t - T_{i,j}^{t-\Delta t}}{\Delta t} \right) \quad (2)$$

where $T_{i,j}$ is the temperature of the roll in the axial direction i and radial direction j ; $T_{i,j}^t$ is the temperature of the roll at axial direction i and radial direction j at time t ; $T_{i,j+1}$ and $T_{i,j-1}$ are the temperature of the radial upper and lower units of the roll temperature unit; $T_{i+1,j}$ and $T_{i-1,j}$ are the temperature of the radial right and left units of the roll temperature unit; $T_{i,j}^{t-\Delta t}$ is the temperature of the roll at axial direction i and radial direction j separated by time Δt from time t ; Δr is the radial grid center distance; Δz is the axial grid center distance; Δt is the time interval; k is the thermal conductivity of the roll; C_p is the specific heat capacity of cooling water; B is the rolling strip width; R is the roll body radius; r_0 is the radial distance from the energy conservation point to the center of the roll; L is the length of the roll body; L_0 is the total length of the roll; r_n is the roll neck radius; $\alpha_A, \alpha_B, \alpha_C, \alpha_D$

are the heat transfer coefficients between the roll and the high-temperature rolled piece, cooling water, roll bearing, and indoor air, respectively.

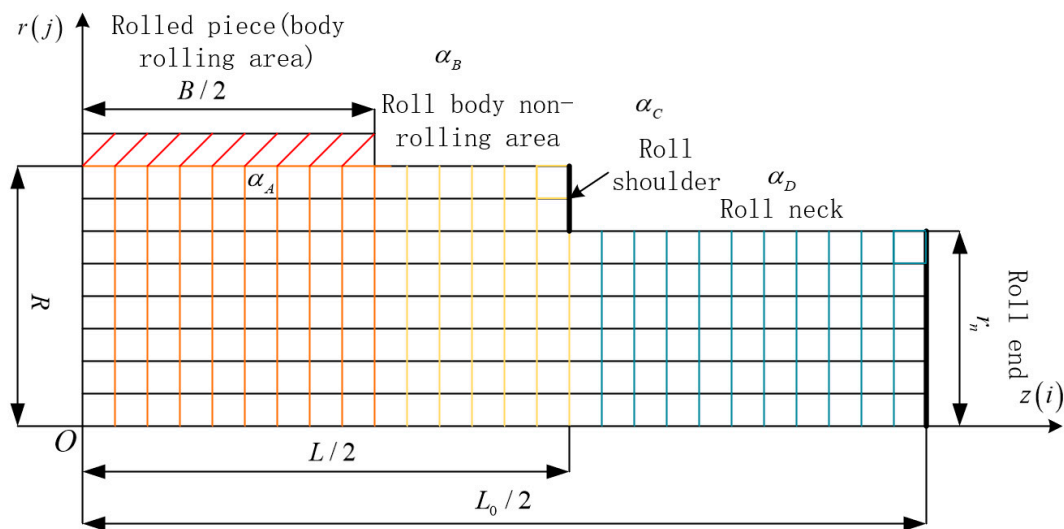


Figure 2. Schematic diagram of work roll mesh division and boundary conditions. The red unit area is the rolled piece, the orange unit area is the body rolling area, the yellow area is the non-rolling area, the blue area is the roll neck, the thick lines are the roll shoulder and roll end in the figure.

2.3. Calculation and Processing of Boundary Conditions

In the course of the rolling process, the work rolls remain in continuous contact with the surrounding mediums such as the high-temperature rolling stock, air, cooling water, and backup rolls. This interaction results in a transfer of heat between the work rolls and the surrounding medium, involving both heat flow input and output. In the context of hot rolling, the primary source of heat input to the work roll is the contact heat conduction occurring between the work roll and the rolled piece, as well as the frictional heat generated between the rolled piece and the work roll. Additionally, the plastic deformation heat produced by the rolled piece contributes to the overall heat input. Conversely, the heat taken away from the work roll is primarily attributed to the convection process between the cooling water and the roll surface, constituting a significant portion of heat exchange. Before delving into the calculations of heat conduction, it is imperative to establish the boundary conditions of the work roll. This involves a comprehensive study of the relationship between the work roll and the surrounding medium. The equation for the boundary conditions of the roll temperature field is elucidated in Equation (3) [25]. Figure 2 illustrates the specific boundary conditions for each part of the work roll.

$$\begin{cases} \alpha_A(T - T_A) + \alpha_B(T - T_B) = -\lambda \frac{\partial T}{\partial r} & (r = R, B/2 \geq z \geq 0) \\ \alpha_B(T - T_B) + \alpha_C(T - T_C) = -\lambda \frac{\partial T}{\partial r} & (r = R, L/2 \geq z \geq B/2) \\ \alpha_C(T - T_C) + \alpha_D(T - T_D) = -\lambda \frac{\partial T}{\partial z} & (z = L/2, R \geq r \geq r_n) \\ \alpha_C(T - T_C) + \alpha_D(T - T_D) = -\lambda \frac{\partial T}{\partial r} & (r = R, L_0/2 \geq z \geq L/2) \\ \alpha_C(T - T_C) = -\lambda \frac{\partial T}{\partial z} & (z = L_0/2, r_n \geq r \geq 0) \end{cases} \quad (3)$$

where T_A, T_B, T_C, T_D are temperatures of the rolled piece, cooling water, roll bearings, and indoor air.

In the context of the rolling process of the work roll body, Newton’s cooling law replaces the external nodes of the roll, while Fourier’s law describes the heat conduction within the roll. Additionally, adhering to the principles of energy conservation, the difference equations corresponding to the boundary grid points of the non-rolling part of the

work roll, the roll shoulder part, the roll neck part, and the roll end part are formulated. The non-rolling section of the roll body is represented by distinct equations for the corner nodes connecting the roll shoulder, roll neck, and roll end parts. Equation (3) is the boundary condition from the center of the roll surface to the center point of the roll center axis. The left side of the equation is the form of Newton's cooling law for the heat flow input within this range. The right side of the equation is the partial differential form of the temperature field with respect to coordinates. The resulting set of differential equations, encompassing all grid points and corner nodes, constituting a linear equation system utilized to solve for the temperature field of the work roll. After a period of time Δt , the equation system is solved once to obtain the transient temperature field of the work roll. The concept of addressing the backup roll is analogous to that of the work roll, with the only distinction lying in the differential equation governing the contact region between the backup roll and the work roll. In this context, the boundary condition is substituted with the temperature of the high-temperature rolled piece, determined by the body temperature of the work roll.

2.4. Hot Roll Crown Model

Assuming that the roll is an infinitely long cylinder, its temperature exhibits an extreme distribution relative to the roll. If we consider the initial temperature of the roll to be $T_0(r, z)$, the thermal roll profile is generated by the thermal expansion of the roll [26]. The non-uniformity of the roll temperature distribution will cause the roll crown to be unevenly distributed along the roll body. The inconsistent axial crown of the roll will cause the strip rolling shape to be unevenly distributed along the width direction, which is also the significance of research on the roll temperature field and hot roll crown.

$$u_t = 2(1 + \nu_p) \frac{\beta_t}{R} \int_0^R (T(r, z) - T_0(r, z)) r dr \quad (4)$$

where u_t is the hot roll profile distribution; β_t is the thermal expansion coefficient; ν_p is the Poisson ratio; T is the roll temperature distribution.

2.5. Cooling Water Section Cooling System

According to related research on the heating and cooling boundary conditions of the roll during the rolling process [27,28], in the realm of hot continuous rolling mills, the intersection between the work roll body and the cooling water gives rise to surface heat exchange, primarily manifested through convective heat transfer. Convection heat transfer refers to the process of transferring heat energy between flowing fluids and solid walls due to temperature differences when they come into direct contact. The involvement of cooling water in convection heat transfer is a primary factor influencing the temperature distribution of the roll. This intricate process is subject to diverse factors influencing the fluid heat transfer coefficient, including fluid flow rate, dynamic viscosity, specific heat capacity, and others. Drawing from analogous theoretical frameworks, we built upon established principles to devise an influence function that characterizes the impact on cooling water heat exchange. This function was derived through meticulous experimentation [29].

$$k_w = \alpha (C_p \mu)^\beta \left(\frac{\lambda_w^3}{d} \right)^a \left(\frac{v}{\mu} \right)^b \quad (5)$$

where k is the cooling water convective heat transfer coefficient; v is the cooling water flow rate; λ_w is the thermal conductivity of the cooling water; d is the equivalent diameter of the cooling water tank; μ is the dynamic viscosity of the cooling water; α, β, a, b is the water cooling coefficient. The cooling water coefficient is a fitting value obtained from the actual measurement results of the test.

In the mathematical model of the convective heat transfer coefficient for cooling water established earlier, a specialized segmental cooling water control system has been incorporated into the temperature field and hot roll crown calculation program. This system,

illustrated in Figure 3, involves the establishment of an array $\nu[i]$ for the cooling water flow rate ν in the formula. By implementing this system, the flow rate of the cooling water in each section of the roll body can be precisely controlled. Consequently, the cooling water temperature and flow rate are adjusted as dual variables, enabling accurate regulation of the unit roll body temperature during the rolling process. This approach enhances the overall control and efficiency of hot continuous rolling mills. In terms of hardware, as shown in Figure 3, two rows of cooling pipe beams are arranged in the rolling exit direction, while one row is positioned in the inlet direction. Each row of cooling beams is equipped with a specific number of cooling water nozzles based on the varying lengths of the rolls. This system comprises nine nozzles, including controllable ones on both sides and a centrally located, normally open, nozzle. As depicted in Figure 3b, left view, all nozzles possess the capability to adjust both the temperature and injection angle of the cooling water. Furthermore, the controllable nozzles can regulate the outlet flow rate and individual flow rate for each nozzle separately, thereby meeting both software and hardware requirements for controlling water flow rate within this system. Consequently, achieving segmented cooling control through precise adjustment of cooling water becomes attainable.

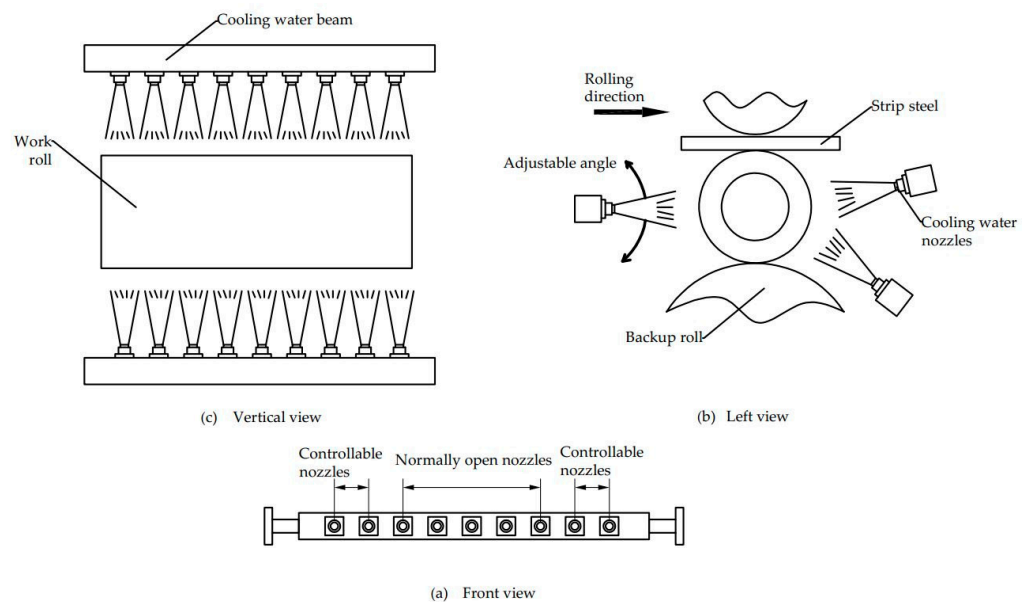


Figure 3. Cooling water bracketed cooling system positioning.

3. Results and Discussion

3.1. Numerical Simulation and Practical Application of Temperature Field and Hot Roll Crown

Based on the established model for the roll temperature field, a software program was developed to calculate both the roll temperature field and the hot roll shape. Figure 4 illustrates the calculation process, demonstrating the superimposition of the roll temperature field and hot roll shape against the number of steel coils.

Under identical rolling conditions, specifically maintaining consistent parameters such as the quantity of rolled steel coils and the cooling water flow rate, a comparative analysis was conducted between simulation calculations and the actual production data obtained onsite, as illustrated in Figure 5.

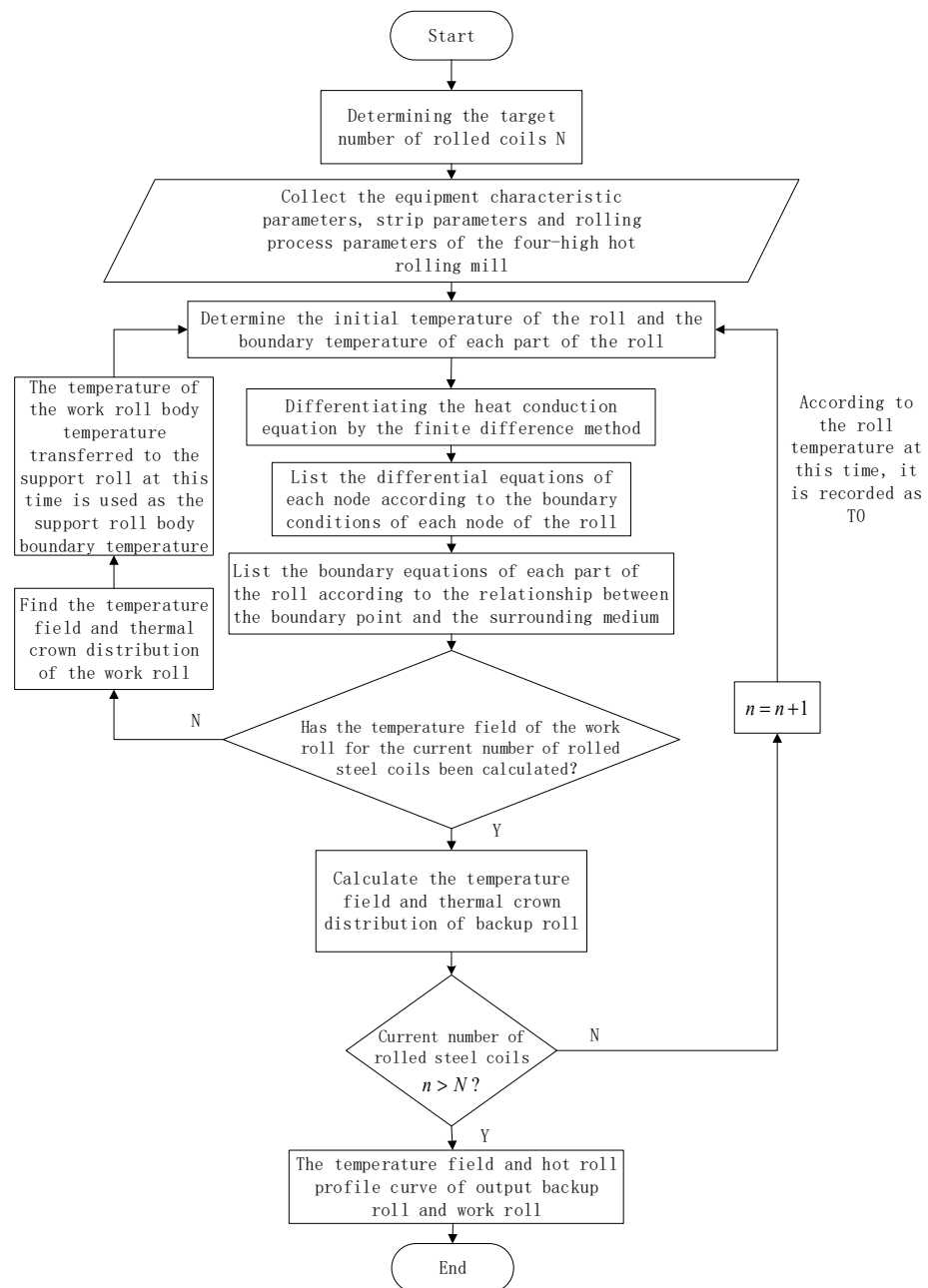


Figure 4. Flow chart of the calculation of the roll temperature field and hot roll shape.

As depicted in Figure 5, the temperature field, as calculated by the model, aligns closely with the field data, demonstrating consistency with the results of the hot roll shape calculations. In instances where the model predictions diverge from the measured field results, adjustments are imperative, grounded in the material parameters of the incoming slab and the current status of the roll. This necessitates appropriate modifications to the heat transfer coefficient, cooling water flow rate, and the roll crown, accounting for wear, roll bending, and other influencing factors. In the realm of hot continuous rolling mills, the accuracy of the temperature field and hot roll crown predictions plays a pivotal role in optimizing operational efficiency. As the temperature field and thermal roll shape prediction software calculates the roll's temperature in its machine state, while onsite data represent the temperature measured after removing the roll from the machine, it was observed that the software calculation results slightly exceed those obtained from onsite measurements. This deviation aligns seamlessly with the actual onsite scenario.

The harmonization between onsite production results and the simulated values generated by the roll temperature field and hot roll shape modeling software serves as compelling evidence for the correctness and efficacy of the employed temperature field and hot roll shape software. This correlation underscores the software's ability to reflect real-world conditions, thereby affirming its practical utility in the realm of hot continuous rolling mills. In the calculation model for the roll temperature field and hot roll profile, particular attention is given to the impact of the roll temperature field and the hot roll profile in relation to the rolling mileage of the roll. The relevant models for the roll temperature field and hot roll profile are cyclically superimposed, enhancing the simulation to yield calculated values that closely align with the actual production conditions. The temperature field of the roll and the contour of the hot roll evolve with the number of coils of the rolled strip. This evolution is assessed by comparing the temperature field of the roll under different cooling conditions, specifically when using the segmental cooling water system versus the cooling water system, while maintaining the same cooling water flow rate. Variations in volume, such as volume 1, volume 5, and volume 10, were examined to provide a comprehensive understanding of the thermal and profile changes in hot continuous rolling mills, the results of which are shown in Figures 6–9.

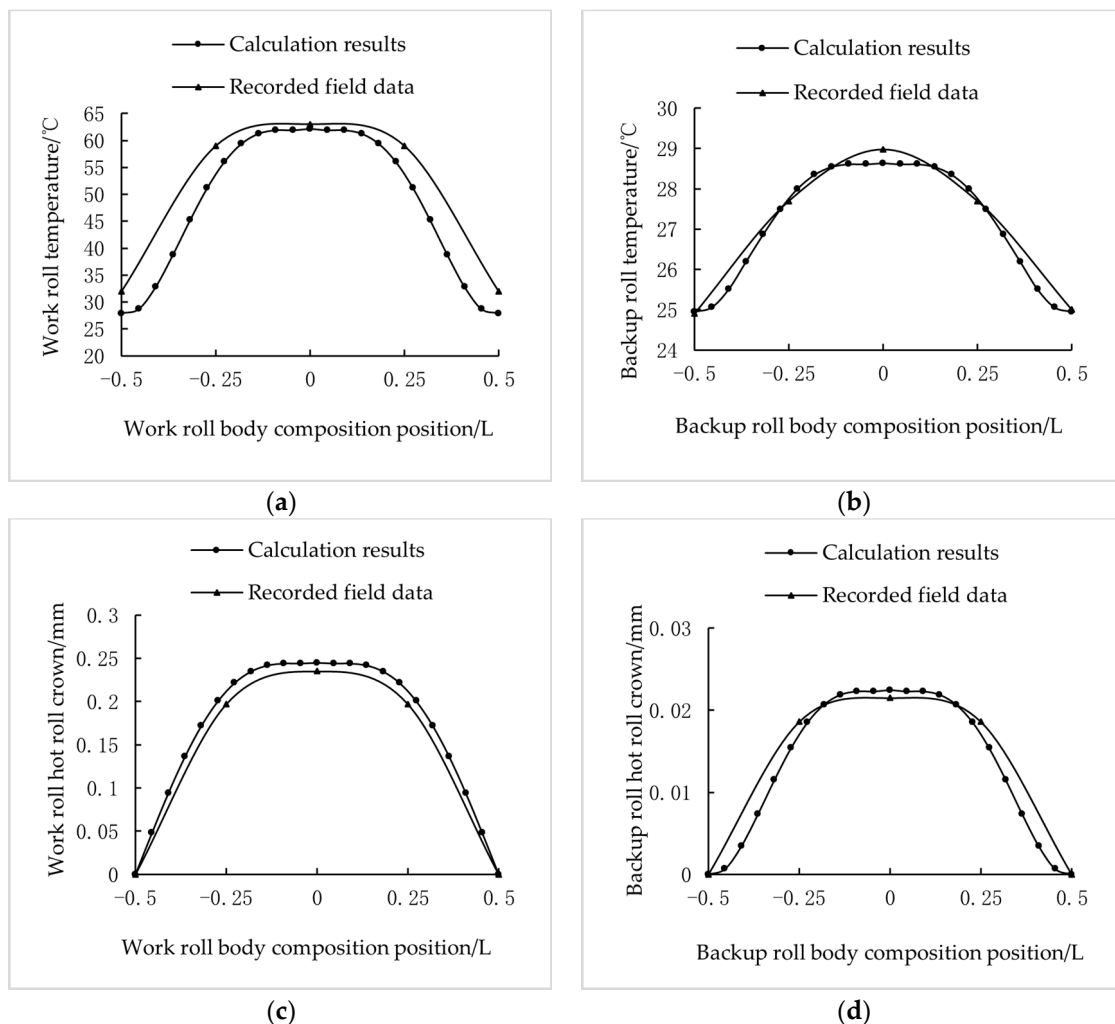


Figure 5. Comparing the curves of the calculation results and field data. (a) Work roll temperature field comparison; (b) backup roll temperature field comparison; (c) work roll hot roll crown comparison; (d) backup roll hot roll crown comparison.

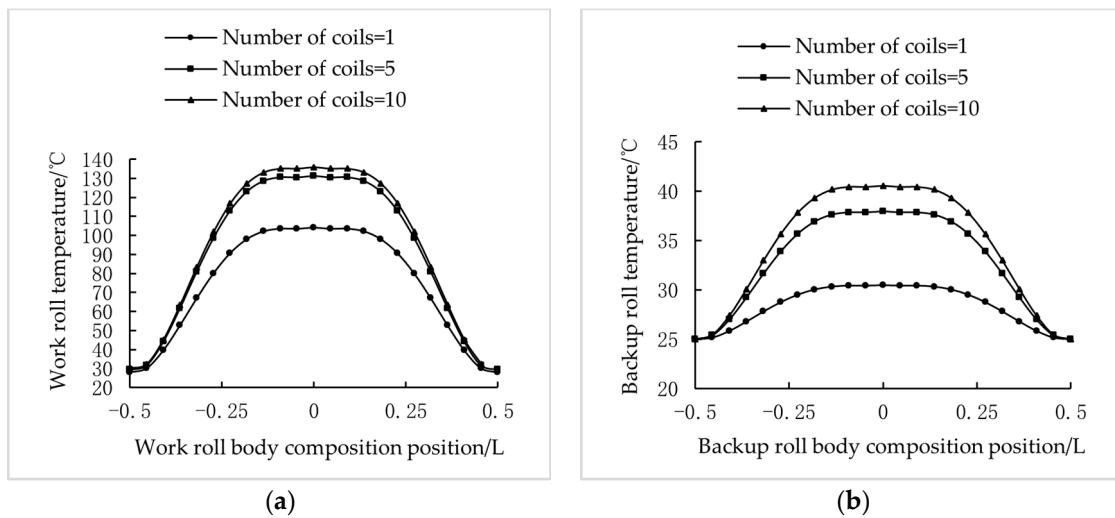


Figure 6. Roll temperature field without cooling water. (a) Change curve of the work roll temperature field with different numbers of rolling strip coils; (b) change curve of the backup roll temperature field with different numbers of rolling strip coils.

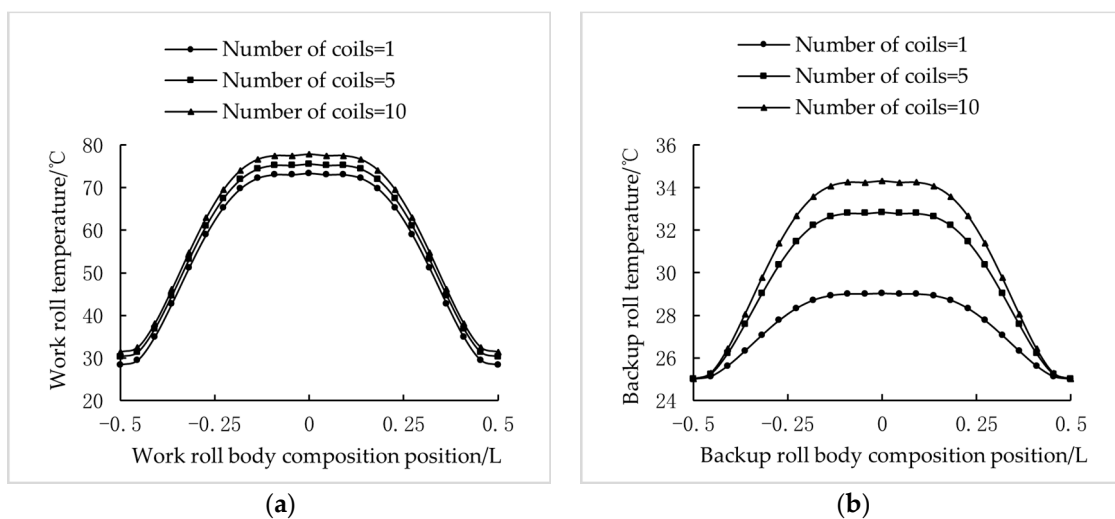


Figure 7. Roll temperature field with cooling water. (a) Change curve of the work roll temperature field with different numbers of rolling strip coils; (b) change curve of the backup roll temperature field with different numbers of rolling strip coils.

The investigation focuses on monitoring the temperature field and the contour of hot rolls in hot continuous rolling mills in relation to the number of rolled steel coils. This study considers the impact of a dedicated cooling water system for both work rolls and backup rolls, as well as a comparison with an unloaded cooling water system. In the initial 10 rolls of the rolling process, the temperature and thermal crown of the work rolls exhibit an upward trend. Subsequently, after approximately 8–10 rolls, both the temperature and thermal crown stabilize, with a slight subsequent temperature increase. During the rolling process, the roll temperature will eventually reach a stable value due to the involvement of cooling water and heat dissipation from room temperature air. In practical production, it is common practice to initially roll with preliminary materials in order to ensure that the rolling mill achieves a stable state before normal production commences. The number of steel coils required before reaching this stable state can serve as a reference for onsite production, thereby ensuring product quality and minimizing waste generation. After comparing Figures 6 and 7, it was observed that the inclusion of cooling water to the work roll resulted in a significant decrease in the maximum rolling temperature from 136 °C to

38 °C. Similarly, upon analyzing Figures 8 and 9, it was evident that the addition of cooling water led to a notable reduction in the maximum thermal crown of the work roll from 0.67 mm to 0.33 mm. The implementation of the cooling water system markedly reduces the overall temperature of the rolls. It is evident from comparison of Figures 7 and 9 that minimal alterations are observed in both the temperature and shape of the hot rolls as the number of coils rolled increases. The maximum temperature of the support roller dropped from 41 °C to 34 °C, and the maximum thermal crown of the support roller dropped from 0.1 mm to 0.05 mm. In Figures 6b–9b, irrespective of the involvement of the cooling water system, a notable variation in temperature and shape of the hot rolls occurs as the number of steel coils increases, with a maximum temperature difference of 10 °C observed for the support roller and a crown difference of 0.07 mm. The effect is reduced compared to the impact observed with work rolls and is not as pronounced. This disparity can be attributed to the direct addition of the cooling water system to the work rolls; however, due to the contact between the work rolls and backup rolls during the rolling process, a portion of the cooling water affects the backup rolls. This outcome aligns with practical field observations.

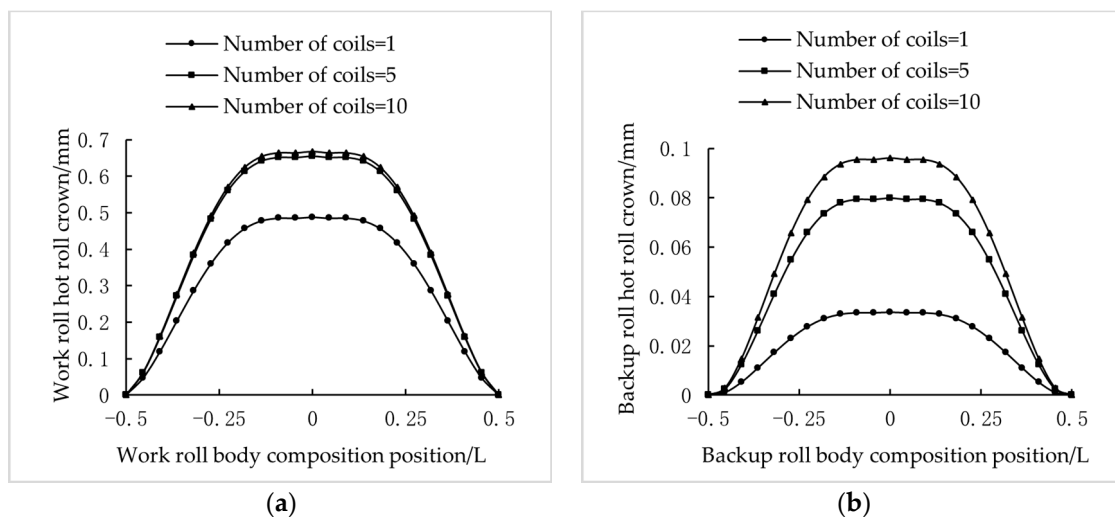


Figure 8. Hot roll crown without cooling water. (a) Change curve of the work roll hot roll crown with different numbers of rolling strip coils; (b) change curve of the backup roll hot roll crown with different numbers of rolling strip coils.

Next, by controlling the flow rate of the cooling water in the system, compare and observe the changes of the temperature field of the work roll and the backup roll and the shape of the hot roll at flow rates of 1.0 m/s, 1.2 m/s, and 1.5 m/s, respectively.

Based on the simulated calculation results for the roll temperature field and the hot roll shape model, the cooling water flow rate exhibits a pronounced impact on both the roll temperature field and the resulting hot roll profile. As illustrated in Figure 10, an increase in the cooling water flow rate correlates with a decrease in the temperature of both the work rolls and backup rolls during the rolling process, consequently leading to a reduction in the resultant hot roll profile. The cooling water system effectively regulates the flow rate and temperature by segmenting the cooling beam nozzles, thereby achieving precise control over both individual roll temperatures and overall temperature. As depicted in Figure 10, it is evident that the three distinct cooling water flow rates successfully limit the maximum work roll temperature to 73 °C, 62 °C, and 52 °C, respectively. Additionally, this approach ensures controlled thermal crowns of 0.30 mm, 0.25 mm, and 0.16 mm, for each respective case, while also extending its benefits to support roller regulation with similar outcomes achieved. Simultaneously, the noticeable temperature variation in the working rolls, compared to the backup rolls, aligns with the segmented cooling system's actual design [30].

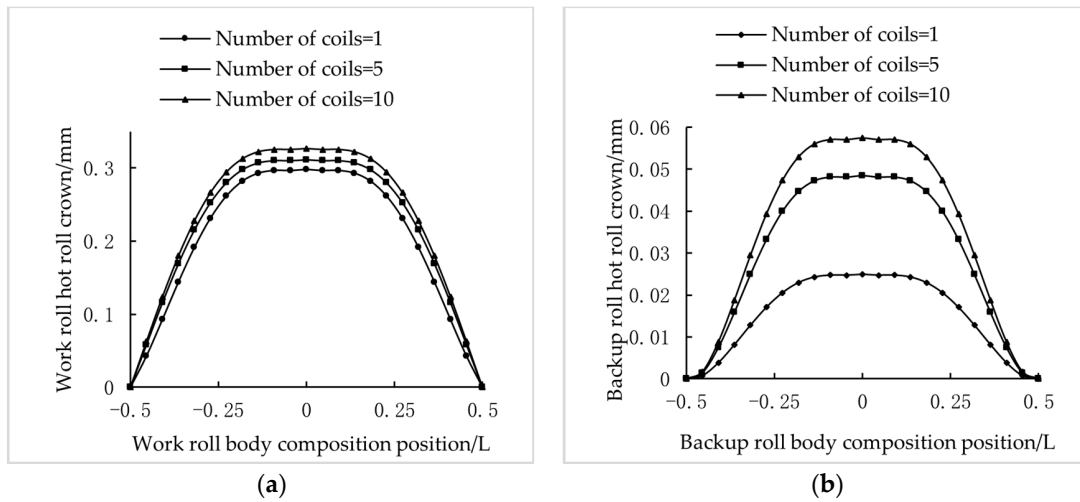


Figure 9. Hot roll crown with cooling water. (a) Change curve of the work roll hot roll crown with different numbers of rolling strip coils; (b) change curve of the backup roll hot roll crown with different numbers of rolling strip coils.

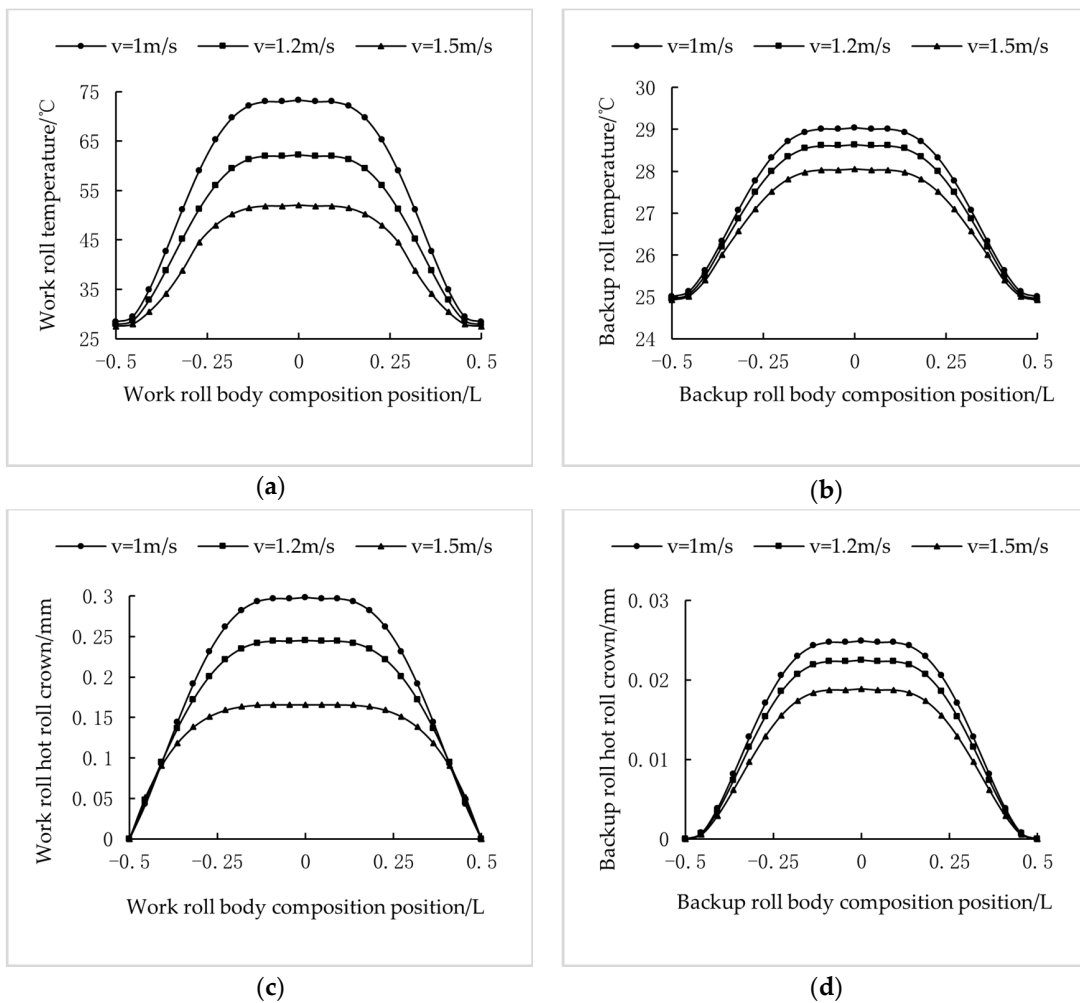


Figure 10. Roll temperature field and hot roll crown at different speeds. (a) Change curve of the temperature field of the work roll under different flow rates; (b) change curve of the temperature field of the backup roll under different flow rates; (c) change curve of the hot roll crown of the work roll at different flow rates; (d) change curve of the hot roll crown of the backup roll at different flow rates.

3.2. Finite Element Numerical Simulation Verification

Through simulation, it was observed that, during the roll's operation at a rolling speed of 4 m/s, it reaches the steady state of the temperature field. The temperature field distribution is illustrated in Figure 11. After completing the calculation, 19 measuring points were evenly distributed along the roll body during the rolling steady state. The temperature calculation values at these measuring points were extracted to generate the temperature distribution curve along the direction of the roll body, as illustrated in Figure 12. The average temperature of the roll surface in the non-rolling area is 29.7 °C, while in the rolling area, it averages at 78.8 °C. Notably, there exists a temperature transition area approximately 123.7 mm wide between these two regions [31].

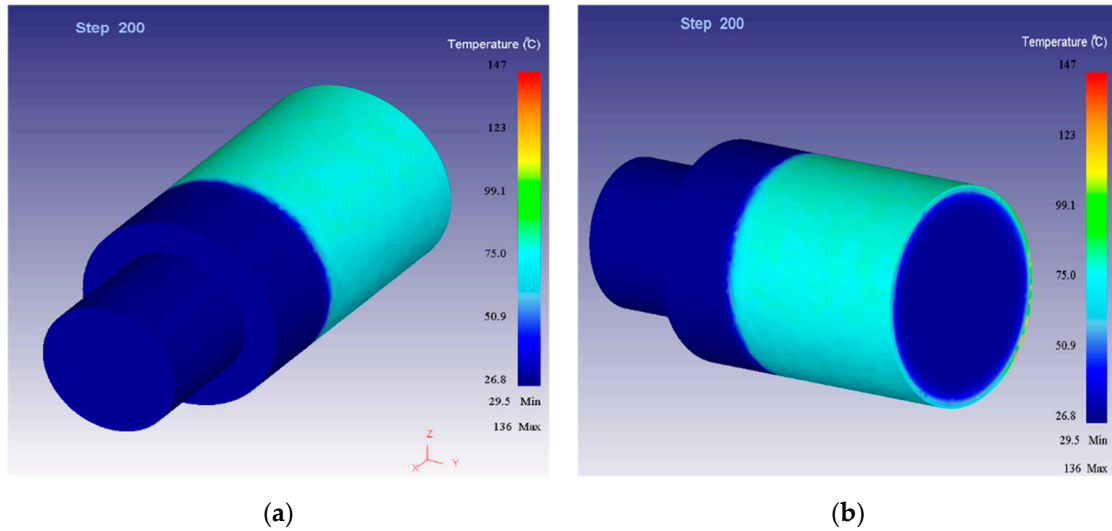


Figure 11. Rolling steady state temperature field distribution. (a) Roll front view; (b) roll rear view.

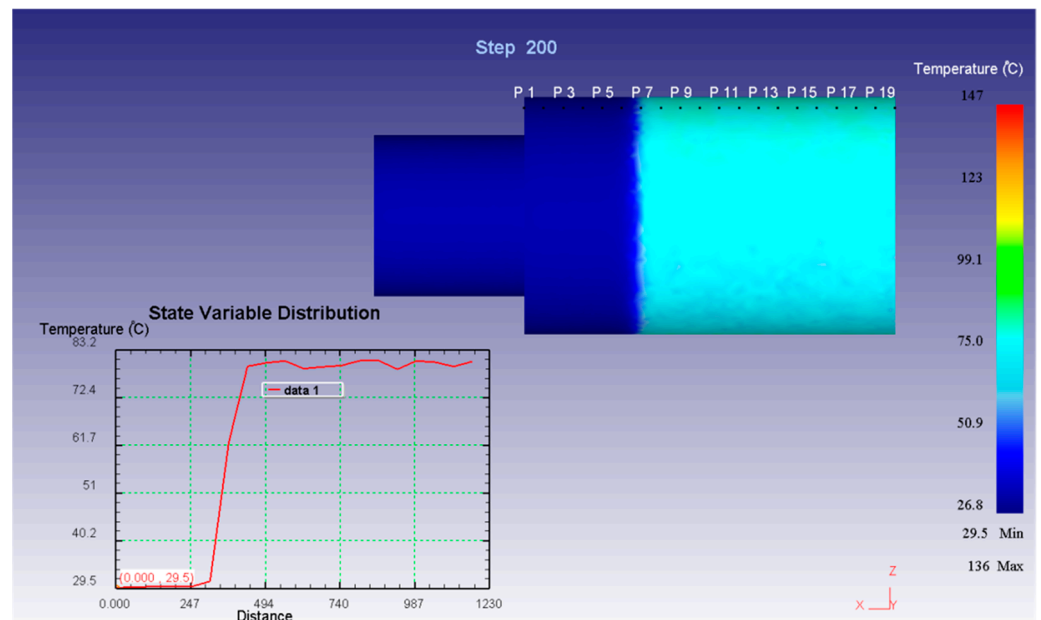


Figure 12. Finite element analysis results for the roll temperature field.

Based on the finite element model of the work roll, the calculated temperature distribution at each node of the roll aligns closely with the simulated values obtained through the established temperature field and thermal roll shape software. Consequently, the computed values derived from the finite element model exhibit consistency with those of the roll.

This alignment between the temperature field and simulation values, as determined by the thermal roll shape software, substantiates the accuracy and validity of both the temperature field and the thermal roll shape model. In the future, it is imperative to achieve a unified approach encompassing theories, models, numerical simulations, and field applications while concurrently optimizing and enhancing the accuracy of the software. Conversely, in terms of hardware, the efficacy of the segmented cooling water control system hinges upon its seamless integration and harmonization with the software.

4. Conclusions

(1) The finite difference method was employed to comprehensively account for the complex boundary conditions and heat transfer phenomena within hot continuous rolling mills. This includes considerations for the interaction between the rolling piece and the work roll, the plastic deformation heat of the rolling piece, air cooling, contact heat conduction between the work roll and the rolling piece, as well as convective heat transfer between the cooling water and the roll. Consequently, a thermal method was developed, presenting a theoretical calculation model for the temperature field and hot roll profile tailored to hot rolling and finishing rolling processes.

(2) Additionally, the introduction of a segmented cooling water system, coupled with a meticulous consideration of the precise cycle iteration effect of the number of rolling steel coils on the temperature field, reveals noteworthy findings. The study concludes that, under flow rates of 1.0, 1.2, and 1.5 m/s, respectively, the maximum temperature difference at the middle point of the work roll is 21.3 °C, resulting in a maximum roll crown difference of 0.132 mm. Similarly, the maximum temperature difference at the middle point of the support roll is 0.98 °C, with a corresponding maximum roll crown difference of 0.006 mm. Notably, the study identifies that the number of rolled steel coils peaks around 10 coils, indicating a relative temperature rise in the steady state.

(3) Furthermore, comparative analysis of the model-calculated results and the actual production data reveals a high level of accuracy. The calculated model predicts a temperature of 62.1 °C, closely aligning with the actual onsite data of 63 °C. The simulated temperature values for both the work roll and the support roll exhibit excellent agreement with the actual measured values, demonstrating that the model's calculations meet practical engineering requirements.

Author Contributions: Conceptualization, Z.L. and S.A.E.; data curation, S.A.E. and S.K.; formal analysis, L.L. and B.Y.; methodology, Z.B.; validation, Z.L., S.K. and B.Y.; writing—original draft, Z.L.; writing—review and editing, L.L. and Z.B. All authors have read and agreed to the published version of the manuscript.

Funding: This research was funded by the Science and Technology Research Project of Higher Education Institutions in Hebei Province, the Major Scientific and Technological Achievements Transformation Project of Hebei Province, the Funding Project of Central Guiding for Local Science and Technology Development, the Hebei Province Science and Technology Research and Development Plan-Science and Technology Support Plan Project and the Basic Project of Higher Education Institutions in Liaoning Province, grant numbers CXY2023012, 22281001Z, 236Z1024G, 23280101Z, and LJKZZ20220040.

Data Availability Statement: The original contributions presented in the study are included in the article, further inquiries can be directed to the corresponding author.

Conflicts of Interest: The authors declare no conflicts of interest.

References

1. Li, X.T.; Zhang, Y.D. Comprehensive optimization technology of rolling temperature for seven stand hot strip mill. *Iron Steel* **2023**, *58*, 104–110.
2. Xu, J.; Guan, B. Tailoring the microstructure and mechanical properties of Cu–Fe alloy by varying the rolling path and rolling temperature. *J. Mater. Res. Technol.* **2023**, *27*, 182–193. [[CrossRef](#)]

3. Guo, Z.F.; Xu, J.Z. Temperature Field and Thermal Crown of Work Rolls on 1700 Hot Strip mill. *J. Northeast. Univ. (Nat. Sci. Ed.)* **2008**, *4*, 517–520.
4. Qu, F.Q.; Li, X. Thermal crown of cold rolling work roll and its effect on strip shape. *China Metall.* **2022**, *32*, 84–93.
5. Li, B.Q.; Fan, X. Parameter optimization of shape setting model and application of control technology. *Iron Steel* **2019**, *54*, 41–47.
6. Meng, L.M.; Ding, J.G. Prediction of roll wear and thermal expansion based on informer network in hot rolling process and application in the control of crown and thickness. *J. Manuf. Process.* **2023**, *103*, 248–260. [[CrossRef](#)]
7. Wei, C.; Song, S.X. Evaluation of elastic-plastic deformation in HSS work roll under coupling of residual stress thermal stress and contact stress during hot rolling. *Mater. Today Commun.* **2022**, *33*, 104613. [[CrossRef](#)]
8. Atack, P.A.; Robinson, I.S. Control of thermal camber by spray cooling when hot rolling aluminum. *Iron Steel* **1996**, *23*, 69–73.
9. Serajzadeh, S.; Mucciardi, F. Modeling the work-roll temperature variation at unsteady state condition. *Model. Simul. Mater. Sci. Eng.* **2003**, *11*, 179–194. [[CrossRef](#)]
10. Sonboli, A.; Serajzadeh, S. A model for evaluating thermal mechanical stresses within work-rolls in hot-strip rolling. *J. Eng. Math.* **2012**, *72*, 73–85. [[CrossRef](#)]
11. Chen, B.G.; Chen, X.L. Prediction of work roll thermal deformation with finite element method on hot strip mill. *Iron Steel* **1991**, *8*, 40–44.
12. Wang, J.; Cao, Y. Finite element analysis on temperature field of work roll in hot rolling strip mill. *Hot Work. Technol.* **2013**, *42*, 102–104.
13. Kong, X.W.; Li, R.L. Fem Calculation of Temperature Field and Axial Thermal Crown for Work Roller. *J. Iron Steel Res.* **2000**, *12*, 51–54.
14. Jiang, M.; Li, X.; Wu, J.; Wang, G. A precision on-line model for the prediction of thermal crown in hot rolling processes. *Int. J. Heat Mass Transf.* **2014**, *78*, 967–973. [[CrossRef](#)]
15. Chen, S.X.; Li, W.G.; Liu, X.H. Thermal crown model and shifting effect analysis of work roll in hot strip mills. *J. Iron Steel Res. Int.* **2015**, *22*, 777–784. [[CrossRef](#)]
16. Li, X.D.; Liu, X.D. Research on the hot roll shape and the cooling system of the hot mill. *Metall. Equip.* **2005**, *5*, 1–4+56.
17. Hiremath, P.; Sharma, S. Effect of post carburizing treatments on residual stress distribution in plain carbon and alloy steels—A numerical analysis. *J. Mater. Res. Technol.* **2020**, *9*, 8439–8450. [[CrossRef](#)]
18. Kumar, A.; Rath, S.L. Simulation of plate rolling process using finite element method. *Mater. Today Proc.* **2021**, *42*, 650–659. [[CrossRef](#)]
19. Chrysanidis, T. Experimental and numerical research on cracking characteristics of medium-reinforced prisms under variable uniaxial degrees of elongation. *Eng. Fail. Anal.* **2023**, *145*, 107014. [[CrossRef](#)]
20. Guo, W.T.; He, A.R. Research on work roll thermal contour model in hot strip mill based on the turning direction two dimensional difference method. *Metall. Equip.* **2009**, *1*, 20–23.
21. Li, Y.W.; Yan, S.L. Deformation behavior of high-chromium cast iron / low-carbon steel laminates based on hot rolling and finite element simulation. *Vacuum* **2023**, *214*, 112218. [[CrossRef](#)]
22. Yu, H.; Guo, Z.Y. Study on the thermal profile of work rolls for four high mills. *Shanghai Met.* **2005**, *1*, 26–30.
23. Wang, G.D. *Plate Shape Control and Plate Shape Theory*; Metallurgical Industry Press: Beijing, China, 1980; pp. 10–86.
24. Li, J.H.; Lian, J.C. Prediction Model of Temperature Field and Crown of Work Roll for Hot Strip Mill. *J. Iron Steel Res.* **2003**, *6*, 25–28.
25. Sun, Y.K. *Model and Control of Hot Strip Rolling*; Metallurgical Industry Press: Beijing, China, 2007; pp. 56–106.
26. Beeston, J.W.; Edwards, W.J. Thermal Camber Analysis in Cold Rolling. *Iron Steel Inst.* **1973**, *5*, 320–324.
27. Onah, O.T.; Ekwueme, B.N. Improved design and comparative evaluation of controlled water jet impingement cooling system for hot-rolled steel plates. *Int. J. Thermofluids* **2022**, *15*, 100172. [[CrossRef](#)]
28. Zhang, R.; Li, Z.L. Numerical simulation of multi-array spray cooling for hot rolled seamless steel pipes. *Int. J. Heat Mass Transf.* **2024**, *221*, 125017. [[CrossRef](#)]
29. Lu, H.M.; Chen, Y.Y. *Mechanical Engineering Material Properties Data Sheet*; China Machine Press: Beijing, China, 2007; pp. 441–726.
30. Li, Z.Z.; Liu, L.X. Research on roll temperature field and hot roll crown of hot continuous rolling mills. *Iron Steel* **2023**, *1*, 1–10.
31. Raja, N.; Kumar, A. Finite element modelling and microstructural correlation of hot forged Al-Zn-Mg-Cu alloy (T6) using DEFORM-3D. *Mater. Today Proc.* **2023**, *in press*. [[CrossRef](#)]

Disclaimer/Publisher’s Note: The statements, opinions and data contained in all publications are solely those of the individual author(s) and contributor(s) and not of MDPI and/or the editor(s). MDPI and/or the editor(s) disclaim responsibility for any injury to people or property resulting from any ideas, methods, instructions or products referred to in the content.